Original Research

In vivo miRNA delivery in whitefish: Synthetic MiR92b-3p uptake and the efficacy of gene expression silencing

Paweł Brzuzan[1], Maciej Woźny[1], Bogdan Lewczuk[2], Maciej Florczyk[1], Piotr Gomułka[3], Paulina Budzińska[1], Michał Wesołowski[1] and Stefan Dobosz[4]

[1]Department of Environmental Biotechnology, Faculty of Environmental Sciences, University of Warmia and Mazury in Olsztyn, Olsztyn 10-709, Poland; [2]Department of Histology and Embryology, Faculty of Veterinary Medicine, University of Warmia and Mazury in Olsztyn, Olsztyn 10-713, Poland; [3]Department of Ichthyology, Faculty of Environmental Sciences, University of Warmia and Mazury in Olsztyn, Olsztyn 10-719, Poland; [4]Department of the Salmonid Research in Rutki, Inland Fisheries Institute in Olsztyn, Żukowo 83-330, Poland
Corresponding author: Paweł Brzuzan. Email: brzuzan@uwm.edu.pl

Impact statement

The delivery of short snippets of RNA, such as synthetic miRNA agents, is an essential step for achieving RNA-mediated knockdown, which has not been studied in sufficient detail in fish. Our results indicate that a MiR92b-3p mimic may be effectively delivered via intraperitoneal injection to the spleen and the liver of whitefish, and that it likely achieves functionality without causing any apparent toxic effects in the challenged animals. We report the novel finding that the MiR92b-3p mimic reduced the *in vivo* liver mRNA expression levels of its putative pro-apoptotic targets (p53, cdkn1a, and pcna), and important metabolic genes, e.g. *cdo1*. This shows that this methodology of MiR92b-3p mimic transfection *in vivo* may be a useful tool for studies that investigate the molecular pathways that confer pro-proliferative and anti-apoptotic phenotypes or those that regulate intracellular metabolism in fish and other vertebrates.

Abstract

Here, we provide the first report of an efficient method of *in vivo* delivery of MiRNA92b-3p mimic by intraperitoneal injection to whitefish, a Teleost fish. Juvenile whitefish were exposed to synthetic MiR92b-3p suspended in Invivofectamine 3.0 transfection reagent. After 24 and 48 h of the treatment, the blood, liver, spleen, brain, and heart of the fish were sampled to track the uptake of the synthetic miRNA and to assess its specific and off-target effects. RT-qPCR indicated that, within the first 24 h of treatment, MiR92b-3p levels were higher in the blood plasma, liver, and spleen of the injected fish than in the control fish that were administered only solvent vehicle, which was further confirmed by screening the organs with a fluorescently labeled MiR92b-3p probe. We then found that, 48 h after the injection, the mimic decreased the mRNA levels of its putative downstream targets (p53, cdkn1a, and pcna) by approximately 50%, which may indicate that MiR92b-3p was functional. Further profiling of mRNA expression in the liver by RNA sequencing showed perturbations that did not prompt global, specific silencing but instead produced significant differences in expression of a number of genes 48 h after transfection with the mimic. Neither histological nor ultrastructural analyses showed any pathological changes in the liver structure of the exposed fish, and biochemical measurements of the fishes' blood did not differ between the experimental groups. Together, these results indicate that the MiR92b-3p mimic was effectively delivered to the liver of the injected fish, and that the short-term treatment did not cause any apparent toxic effects. This methodology of miRNA mimic delivery has utility not only for the study of miRNA-dependent silencing mechanisms in fish, but also gives reasons to anticipate significant progress in the development of both miRNA diagnostic markers and therapeutic targets in liver injury.

Keywords: cdo1, *in vivo* screening, oligonucleotides mimicking miRNAs, RNA-Seq, transfection, imaging

***Experimental Biology and Medicine* 2019; 244: 52–63. DOI: 10.1177/1535370218824573**

Introduction

RNA interference is a natural cellular process that silences gene expression by promoting the degradation of mRNA or translational repression.[1] MicroRNAs (miRNAs) are small (18 to 24 nucleotides) endogenous non-coding effector RNA molecules with important roles in these processes.[2] Dysregulation in the expression of miRNAs contributes to the occurrence and development of a number of diseases. Reversing pathologic alterations in miRNA expression by delivering miRNA-based drugs is a potential therapeutic

strategy for many malignancies. Carrying miRNA inhibitors into a cell results in silencing of a specific miRNA, whereas the goal of miRNA replacement therapy using synthetic miRNAs (i.e. miRNA mimicking oligonucleotides, mimics) is to achieve, or maintain, the same biological functions as the endogenous miRNAs. In mammals, the hepatic delivery of either class of synthetic nucleic acids has proven to be an excellent strategy for curing metabolic diseases,[3] virus infections,[4] and neuropathy.[5]

In fish, approaches for achieving knockdown are rare and involve mainly small model species. Both kinds of synthetic miRNAs, inhibitors and mimics, have been used as research tools to study the gene functions of different cell types. For example, Cui *et al*.[6] showed that administration of a MiR8159 mimic into miiuy croaker (*Miichthys miiuy*) downregulated the expression of toll-like receptor 13, TLR13, at the transcription level, and confirmed the role of this miRNA in TLR signaling pathway regulation after *Vibrio anguillarum* infection. A study on zebrafish (*Danio rerio*) injected with an miRNA mimic revealed MiR155 to be a potential novel toxicological biomarker for chemical exposure and improved our understanding of the molecular mechanism of toxicity upon fipronil exposure.[7] Mennigen *et al*.[8] using a MiR122-5p antimir, confirmed the role of MiR122-5p in regulating lipid metabolism in rainbow trout (*Oncorhynchus mykiss*). Transcriptome profiling of short-lived killifish (*Nothobranchius furzeri*) suffering from gentamicin-induced renal injury identified apoptosis as a process that was significantly affected upon antiMiR-21 administration.[9] This suggests that MiR-21 acts as a pro-proliferative and anti-apoptotic factor in kidney regeneration in fish.

The successful applications of synthetic miRNAs to resolve problems pertinent to fish biology and immunology, as highlighted in the above studies, prompted us to use RNA interference methods, which revealed a specific, biphasic pattern of microcystin-induced liver injury (MILI) in a teleost fish, whitefish (*Coregonus lavaretus*), as reported previously.[10] In that fish, repeated exposure to microcystin-LR (MC-LR) results in severe liver damage, followed by an unexpected resilience to further exposures to the toxin, leading to regeneration of the damaged liver structure.[10] In these aberrant processes, we found expression of one microRNA, MiR92b-3p, to be substantially reduced in the challenged group.[11] Further functional studies with MiR92b-3p mimics acting on liver transcriptional pathways, conducted *in vivo* on whitefish, might reveal the particular role of this miRNA in the aberrant processes.

In the present work, we first used a MiR92b-3p mimic to replace and increase the number of the miRNA in the liver of healthy fish to assess the *in vivo* efficacy of miRNA uptake and gene silencing. Our main goal was to confirm that the MiRNA92b-3p mimicking oligonucleotides are efficiently delivered into fish by intraperitoneal injection using Invivofectamine 3.0 transfection reagent as a carrier. Then, we were curious about whether MiR92b-3p transfection results in expression changes of putative target genes without generating any unwanted, non-specific effects. High on-target and low off-target activity would indicate that this methodology is appropriate for studying miRNA-dependent, gene silencing mechanisms during MILI. To this end, we exposed fish in three experimental groups and tracked the uptake of the synthetic miRNA in different tissues. Then, using histopathological and ultrastructural analyses, as well as RNA-Seq and qPCR methods, we examined whether non-specific or gene-specific effects occur.

Materials and methods

Fish and experimental design

All animal-related procedures were approved by the Local Ethical Commission in Olsztyn, Poland (resolution No. 44/2016 of 30th November 2016). Juvenile individuals of whitefish (mean ±standard deviation: 29.6 ± 1.6 g, 16.9 ± 0.4 cm) were exposed to a synthetic MiR92b-3p mimic (mirVana^{TM}; Thermofisher Scientific) at a dose of 1 or 0.3 mg·kg^{-1} body weight (MIM-1.0 and MIM-0.3, respectively; $n = 2$ in each group). To increase the delivery efficiency, the mimic was suspended in Invivofectamine 3.0 transfection reagent (Thermofisher Scientific) and injected into the fish intraperitoneally (Supplementary Figure 1(a) and (b)). Fish injected with the *in vivo* transfection reagent alone (IVF; $n = 2$) or phosphate buffer saline (PBS; $n = 3$) served as negative control groups. After treatment, the fish were euthanized and their blood, liver, spleen, heart, and brain were collected at 24 and 48 h, and fixed for further analyses, according to the details described below.

In order to track mimic uptake in fish tissues, we further performed a separate exposure, where additional fish were injected with a synthetic MiR92b-3p mimic 3′-labeled with Alexa Fluor 555 (mirVana^{TM}; Thermofisher Scientific) at a dose of 1 mg·kg^{-1} body weight (MIM-AF; $n = 3$). In this case, fish injected only with the phosphate buffer saline served as a negative control (PBS; $n = 5$). After 24 h of the treatment, the fish were euthanized and their tissues were fixed for further analyses.

Although large numbers of fish in each group would be ideal, the costs involved in the treatment with an IVF carrier (fish with IVF alone, and with IVF suspended mimic), made it impossible to have so many fish in the study. Nevertheless, our preliminary results allowed us to estimate the uptake efficiency, and add to the little that is known about treatment of fish with synthetic miRNAs.

Measurement of MiR92b-3p levels in blood plasma

In order to track the uptake of the synthetic miRNA, blood samples were used to measure MiR92b-3p levels in the plasma of the exposed fish. Briefly, around 0.3 mL of blood was taken from the caudal vein using S-Monovette K3 EDTA (Sarstedt). After collection, the blood was mixed by gently inverting the tube several times and immediately centrifuged at 4000×*g* at room temperature for 5 min. The plasma layer (approximately 100 µL) from the top of the tube was transferred into a fresh tube. Plasma was frozen at −24°C during sample collection, but shipped on dry ice shortly after, and stored at −80°C in the laboratory until RNA extraction.

Total RNA was extracted from 80 µL of plasma sample using a mirVana isolation kit (Life Technologies) according

to the manufacturer's protocol with modifications. After thawing, samples were briefly centrifuged and 10 volumes of initial plasma volume of Lysis/Binding Buffer were added. Samples were vortexed vigorously for 1 min. After that, to normalize sample-to-sample variation in the RNA isolation procedure, an exogenous spike-in control of 3 μL of synthetic 5 nM cel-MiR39-3p (Genomed; Poland) (5′-UCACCGGGUGUAA AUCAGCUUG-3′) was added and mixed. Then, 80 μL of miRNA Homogenate Additive was added and mixed by inverting the tube several times before it was left on ice for 10 min. Next, 800 μL of Acid-Phenol:Chloroform was added and the mixture was vortexed for 1 min. To separate the aqueous and organic phases, the tubes were centrifuged for 5 min at maximum speed (10,000×*g*) at room temperature. About 300 μL of upper phase was then transferred into a fresh tube, avoiding transfer of any interphase. Next, 1.25 volumes of 99.8% ethanol at room temperature were added, mixed thoroughly by pipetting, and the entire solution (including any precipitate) was transferred into individual filter cartridges before centrifugation for 30 s at 10000×*g*. The resulting flow-through was discarded. Initial washing was conducted with 700 μL of Washing Buffer 1, followed by two washes with 500 μL of Washing Buffer 2/3. RNA was eluted from the washed filter cartridges with 40 μL of preheated (95°C) elution solution.

To profile MiR92b-3p expression, we designed a protocol based on polyadenylated RNA and stem-loop reverse transcription.[11–13] miRNA polyadenylation was performed using a polymerase tailing kit (Epicentre). Reactions were prepared with 1 μL of 10× polyadenylate polymerase buffer, 1 μL of adenosine triphosphate (ATP, 10 mM), 0.5 μL of *Escherichia coli* poly(A)polymerase (4 U), 1 μg of small RNA-enriched RNA fraction, and RNase-free water for a final volume of 10 μL. Reaction mixtures were incubated at 37°C for 30 min, followed by 95°C for 5 min to terminate the adenylation, and then transferred directly to ice. Reverse transcription (RT) was then directly carried out using SuperScript IV Reverse Transcriptase (Thermo Scientific; USA). The cDNA synthesis reaction contained polyadenylated RNA from the previous step, 4 μL of 5× RT buffer, 1 μL of 0.1 M DTT, 1 μL of 10 mM dNTP mix, 1 μL of Ribonuclease Inhibitor and of SuperScript IV RT enzymes, and 1 μL of 100 μM universal stem-loop RT primer (5′-CTC ACA GTA CGT TGG TAT CCT TGT GAT GTT CGA TGC CAT ATT GTA CTG TGA GTT TTT TTT TVN-3′). The reaction was carried out at 23°C for 10 min, 55°C for 10 min followed by 10 min in 80°C. Synthesized cDNA samples were diluted (10×), stored at −80°C, and thawed only once, just before the amplification.

Real-time PCR was used to determine the MiR92b-3p levels in the cDNA samples. Reactions were carried out in final volumes of 20 μL, consisting of 10 μL of Power SYBR Green PCR Master Mix (Life Technologies, USA), 0.25 μM of each primer (forward and reverse; Supplementary Table 1), 1 μL of cDNA template and 7 μL of PCR-grade water. Amplification was performed with an ABI 7500 Real-time PCR System thermocycler (Applied Biosystems; USA) with the following conditions: 95°C for 10 min, then 45 cycles of 95°C for 15 s and 60°C for 1 min. The reaction for each sample was carried out in duplicate. No-template controls (NTCs) were included to test for the possibility of cross-contamination. To check the quality of each PCR product, melting curve analyses were additionally performed after each run. Data were normalized to RNU6 as an endogenous reference (Supplementary Table 1), relative to the control group (PBS or IVF) for the respective time-point of the experiment.

MiR122-5p has been shown to be a robust biomarker in early diagnosis of liver injury in fish.[14] Thus, we also determined the plasma level of MiR122-5p in the experimental fish, as previously described in detail.[14]

RNA extraction from solid tissues

Depending on the size, fragments of fish organs (i.e. liver) or entire organs (i.e. spleen, heart, brain) were preserved in RNAlater solution (Sigma-Aldrich; Germany) and stored at −20°C until extraction. RNA was extracted from fragments of these organs (approximately 20 mg) using a mirVana isolation kit (Life Technologies) according to the manufacturer's protocol. Briefly, 200 μL of Lysis/Binding Buffer was added. Samples were vortexed vigorously for 1 min. Then, 20 μL of miRNA Homogenate Additive was added and mixed by inverting the tube several times before it was left on ice for 10 min. Next, 200 μL of Acid-Phenol: Chloroform was added and the mixture was vortexed for 1 min. To separate the aqueous and organic phases, the tubes were centrifuged for 5 min at maximum speed (10,000×*g*). About 200 μL of upper phase was then transferred into a fresh tube. Next, for the enrichment of small RNA species, a 1/3 volume of 99.8% ethanol at room temperature was added, and the entire solution was transferred into individual filter cartridges before centrifugation for 30 s at 10,000×*g*. The filter cartridge was kept for further isolation of RNA fraction depleted of small RNAs, and the obtained flow-through filtrate (containing the small-RNA-enriched fraction) was mixed with 2/3 volume of 99.8% ethanol and transferred into a new filter cartridge and centrifuged. Next, both the filter cartridges (containing the small-RNA-enriched or the small-RNA-depleted fraction) were washed with 700 μL of Washing Buffer 1, followed by two washes with 500 μL of Washing Buffer 2/3. The RNA fractions were eluted separately from the washed filter cartridges with 40 μL of preheated (95°C) elution solution. The small-RNA-enriched samples were used to determine MiR92b-3p levels in the extracted solid tissues according to the RT-qPCR protocol described above for the plasma samples, whereas the small-RNA-depleted samples extracted from the livers were used to verify the mRNA expression of the potential MiR92b-3p targets.

In vivo verification of potential MiR92b-3p target expression

In this study, we were particularly interested in whether the intraperitoneally administered MiR92b-3p mimic has the ability to silence genes that may be its targets during MC-LR induced liver injury and regeneration. Based on our previous studies, we chose p53 tumor suppressor, its downstream effector, cdkn1a, and proliferating cell nuclear

antigen, pcna, which all had shown opposite expression patterns to MiR92b-3p.[10,11] To predict if MiR92b-3p response elements (MRE) occur within 3′ UTRs of the three genes in whitefish, the respective sequences were obtained from Phylofish database,[15] and the RNAhybrid tool[16] was applied. Then, to examine the expression levels of the genes in whitefish liver after 24 and 48 h of exposure to the mimic, we performed an RT-qPCR study. Briefly, the small RNA-depleted samples were used to synthesize cDNA using a SuperScript IV Reverse Transcriptase and Oligo$(dT)_{20}$ primers, according to the manufacturer's protocol (Thermo Scientific). Real-time PCR was performed with primers specific to the respective mRNA sequences (Supplementary Table 1) with reaction conditions as described above. All the expression data were normalized to rpl19 as an endogenous reference, relative to the control sample (PBS or IVF) at a respective time of the experiment. The data were log-transformed and analyzed for the significance of differences between the two experimental groups of fish (control vs. exposed) were assessed using a two-tailed Welch's *t*-test (SPSS Statistics 24; IBM).

Detection of MiR92b-3p using biotin-labeled oligonucleotides

Dharmacon miRIDIAN Mimics (MIR92a-3p and MIR92b-3p) or Thermo Scientific mirVana LNA Mimic (MIR92b-3p) were mixed in increasing amounts (2.82 ng, 28.2 ng, 282 ng) with corresponding volumes of Gel Loading Buffer II (Ambion), and then MQ water was added for a final volume of 30 μL. Additionally, 13 μL of qPCR products or 15 μg of small RNA-enriched RNA, from the control (IVF) and mimic-treated samples (MIM) were prepared as described above. All samples were further denatured at 95°C for 5 min and immediately cooled down on ice to prevent re-annealing. Samples were then separated in a 10% TBE-Urea in 1 × TBE (200 V for 45 min), which first was pre-run end at 250 V for 20 min. Samples were transferred to BrightStar®-Plus Positively Charged Nylon Membrane (Thermo Scientific) in Mini Trans-Blot Cell (Bio-Rad) at 200 mA for 1 h in 1 × TBE. Membrane was washed in 0.5 × TBE and to fix transfer into membrane UV cross-linked for 3 min, followed by baking membranes in an oven at 80°C for 1 h, washed again and pre-hybridized in ULTRAhyb®-Oligo (Thermo Scientific) for 30 min at 42°C. Biotin- 5′-labeled oligonucleotides antisense to mature miRNAs was commercially obtained from Genomed, Poland and hybridized (600 ng) with membrane overnight in 42°C. The Northern blot probes were: MiR92b-3p – AGG CCG GGA CGA GTG CAA TA and U6 snRNA (control) – TAT GTG CTG CCG AAG CGA GCA C. Membranes were visualized the following day using Biotin Chromogenic Detection Kit (Thermo Scientific).

RNA sequencing and de novo assembly of transcripts

To examine the gene specific effects of the treatment, RNA-Seq methods were used to screen the liver transcriptome in PBS, IVF, and MIM-1.0 groups. RNA integrity was evaluated on Agilent Bioanalyzer 2100 with the Agilent 6000 Nano Kit and the samples with RIN > 8 were taken for library preparation with the Illumina TruSeq Stranded mRNA Library Prep protocol. The libraries were sequenced on Illumina HiSeq4000 sequencer (250–300 bp insert cDNA size, PE150, 50M reads, 15Gb).

Quality control of raw sequencing reads was performed with FastQC version 0.11.5 (https://www.bioinformatics.babraham.ac.uk/projects/fastqc). The reads were processed using the Trimmomatic version 0.36 to remove the adapter sequences and low-quality bases.[17] After quality trimming, the selected reads were assembled into the reference genome by using the Trinity version 2.5.1 with default parameters.[18] The number of detected transcripts was 280,709 with an average length of 838 base pairs. Raw reads were mapped to the reference genome using Bowtie2 version 2.3.3.1. The fraction of uniquely aligned reads was between 92% and 93% per sample. The data from this study have been submitted to the NCBI SRA database (accession #SRS3548719 through #SRS3548724). The accession numbers for data from the individual samples, read numbers in the six samples, and concentrations of total RNA in the extracts are given in Supplementary Table 2.

Transcript abundance levels were estimated using the samtools idxstats version 1.3.1 (http://www.htslib.org). The correlation values (Spearman's correlation) between the samples were computed using the raw counts. The results were between 0.854 and 0.896. To identify the transcripts differentially expressed between the experimental groups, *P*-values and fold changes were computed using the edgeR package.[19] Raw counts were normalized using the TMM normalization method. Then, the common, trended, and tagwise dispersions were estimated. A quasi-likelihood negative binomial generalized log-linear model was fit to count data. Statistical tests implemented in edgeR were conducted. To yield lists of differentially expressed mRNAs, the expression threshold was adjusted as $P = 0.05$. For the construction and visualization of Venn diagrams with the numbers of differentially abundant miRNAs, Venn Diagrams software was used (http://bioinformatics.psb.ugent.be/software/details/Venn-Diagrams).

Functional and ontology patterns of predicted orthologs were examined in the set of differentially expressed genes (DEGs), and BLASTx algorithm with default parameters against the SwissProt database, and the non-redundant transcript database (nt) using the BLASTn algorithm. General classification of the Clusters of the DEGs (COGs) by functional panels of categories was carried out using the KOG analysis.[20] Heat maps for differentially expressed genes based on unadjusted *t*-test *P*-values ($P < 0.01$) were calculated, which provided an overall picture of the impact of MiR92b-3p mimic injection on the liver cell transcriptome. For graphical representation of the 20 most frequent Gene Ontology terms in each of three categories, we used TagCloud software (https://www.wordclouds.com).

Hematological and biochemical measurements in blood

In order to investigate whether the treatment with mimic or the Invivofectamine alone caused any non-specific/off-target

or toxic effects, selected hematological and biochemical markers were measured in the fishes' blood. Briefly, approximately 0.3 mL of blood from the caudal vein was taken with a Blood Gas Monovette syringe (Sarstedt; Germany) and a 0.5·30 mm needle (KDM; Germany). The collected blood samples were immediately used to perform the hematological analysis and further to isolate blood plasma, according to the following protocol. The blood sample was transferred into 1.3 mL Li-heparin microtubes (Sarstedt), gently mixed, and centrifuged for 1.5 min at 13,700×*g* (15,800 rpm) using a StatSpin VT with RT12 rotor (Iris Sample Processing, Inc.; USA). After centrifugation, approximately 100 µL of supernatant (the blood plasma) was transferred into sterile Eppendorf tubes and immediately frozen at −24°C. After thawing at room temperature, the plasma samples were analyzed with a Catalyst Dx Chemistry Analyzer (Idexx Lab; USA) using the dedicated test slides (custom panels). Analysis of biochemical measurements included: glucose (GLU), creatinine (CREA), phosphorus (PHOS), calcium (CA), total protein (TP), albumin (ALB) aspartate aminotransferase (AST), alanine aminotransferase (AST), alkaline phosphatase (ALKP), ammonia (NH3). Globulin (GLOB) was calculated by subtracting the albumin from the total protein. Each plasma sample was thawed only once at room temperature and all of the above measurements were performed at once to eliminate the multiple freezing/thawing cycles.

Hematological analysis was performed according to the standard methods described in Svobodova *et al*.[21] in order to determine the erythrocyte count (RBC), hemoglobin concentration (Hb), hematocrit (Ht), mean erythrocyte volume (MCV), mean corpuscular hemoglobin concentration (MCHC), and mean corpuscular hemoglobin content (MCH).

Histochemical staining and histological analysis

The tissue samples were fixed in 4% formaldehyde in phosphate buffer (pH 7.4) for 48 h, washed in water, dehydrated in ethanol solutions and embedded in paraffin using a TP 1020 tissue processor and an EG 1050 embedding station (Leica; Germany). The 6-µm-thick sections prepared with HM 340E microtome (Microm; Germany) were stained with hematoxylin and eosin method (H&E) using an automated multistainer ST 5020 (Leica) and manually cover slipped. The slides were viewed and photographed using an Axioimager Z1 microscope equipped with an MRC5 color digital camera (Carl Zeiss; Germany).

The tissues obtained from the fish injected with the fluorescently labeled MiR92b-3p (MIM-AF) were fixed in 4% paraformaldehyde in 0.1 M phosphate-buffered saline (pH 7.4) for 48 h, rinsed several times with the phosphate buffer, then transferred to a 30% sucrose solution for 48 h and then frozen at −25°C. The tissue blocks were cut using Microm HM 560 cryostat (Carl Zeiss) at a thickness of 12 µm. The slides were viewed and photographed using the Axioimager microscope Z1 equipped with Apotome and the AxioCam HRm digital camera (Carl Zeiss).

Ultrastructural analysis of the liver

The liver samples were fixed in a mixture of 1% paraformaldehyde and 2.5% glutaraldehyde in 0.2 M phosphate buffer (pH 7.4) for 2 h at 4°C, washed and post-fixed in 2% osmium tetroxide for 2 h. After dehydration, the samples were embedded in Epon 812. Ultrathin sections prepared using a Ultracut III ultramicrotome (Leica) were contrasted with uranyl acetate and lead citrate, and then examined with a Tecnai 12 Spirit G2 BioTwin transmission electron microscope (FEI; USA) equipped with two digital cameras: a Veleta (Olympus; Japan) and an Eage 4k (FEI).

Results

Gross observations

During the study, there were no discernible differences between the swimming behavior of the control fish and those exposed to the mimic. No gross changes were observed in the brain, heart, spleen and liver of the fish; the liver was reddish brown and had tender structure.

MiR92b-3p mimic is detected in cellular RNA extracts from the injected fish

When three commercially available microRNA-92 mimics (MiR92a-3p and two MiR92b-3p) were loaded with increasing concentration into the gel and subjected to Northern blot analysis, we noticed a weak miRNA signal for the MiR92a-3p with a probe against MiR92b-3p. In contrast, strong signals of concentration dependent band intensities were detected for the two MiR92b-3p mimics (Supplementary Figure 2(a)). This result confirmed both sensitivity and specificity of the MiR92b-3p probe for detection of the MiR92b-3p mimicking oligonucleotides. Then, we wished to verify whether the elevated levels of MiR92b-3p could be detected in RNA extracts from tissue samples of mimic-treated fish after the reverse transcription procedure with and universal adapter, stem-loop RT primer. We addressed this issue, using the Northern blot-based method for the detection of adapter ligated RT-transcribed MiR92b-3p, by examining the MiR92b-3p signals in control (IVF) and treated (MIM-1.0) liver samples. Indeed, the procedure showed a sharp band in the MIM-1.0 sample, which had an expected length of about 110 nts (63 of stem loop and about 50 nts of double stranded mimic) (Supplementary Figure 2(b)). Together, these results indicated that methods commonly used for detection of changes in miRNA levels were adequate for assessing the efficiency of mimic uptake in whitefish tissues.

MiR92b-3p mimic reaches different tissues in fish body

To track the route of mimic delivery in whitefish, we checked if the mimic injected into the peritoneal cavity of the fish was present in the blood circulation. Indeed, the intraperitoneal injection of the MiR92b-3p mimic led to a marked, ∼60-fold increase of the mimic in the plasma within the first 24 h of the treatment (Figure 1). In comparison to the control group (PBS) from this period, plasma levels of another microRNA – MiR122-5p remained similar

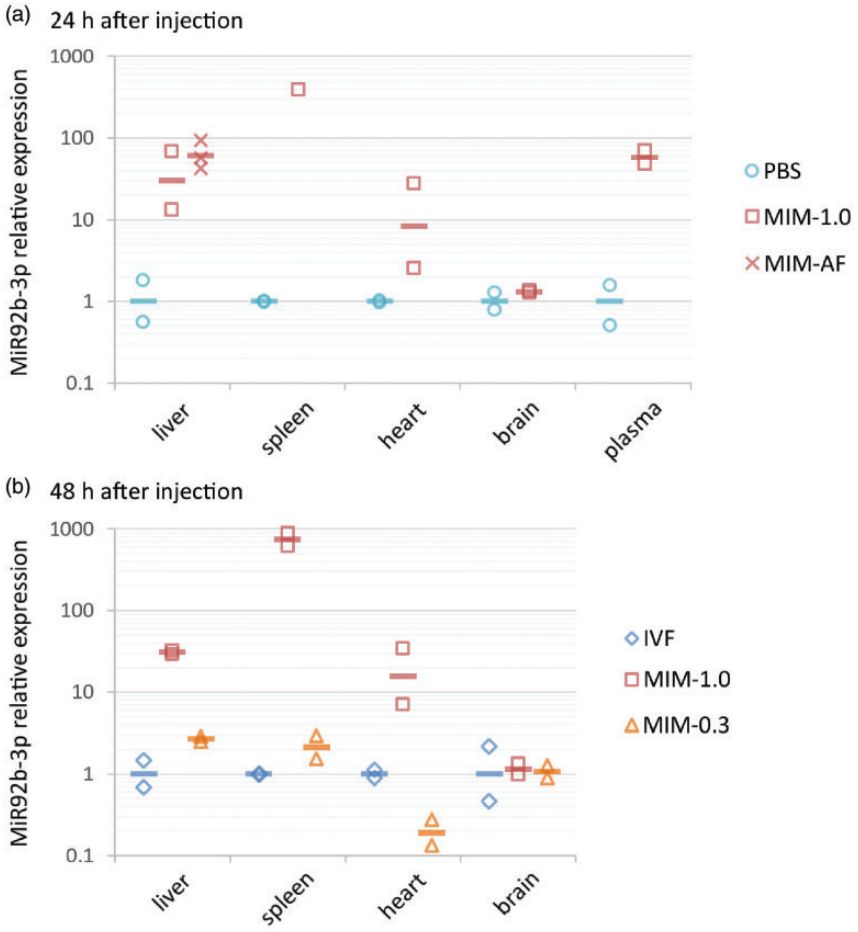

Figure 1. Tissue biodistribution of MiR92b-3p in whitefish 24 h (a) or 48 h (b) after intraperitoneal injection with phosphate buffer saline (PBS), Invivofectamine 3.0 (IVF) vehicle, or MiR92b-3p mimic at dose of 1.0 or 0.3 mg·kg^{-1} (MIM-1.0 or MIM-0.3, respectively), or fluorescently labeled mimic at a dose of 1.0 mg·kg^{-1} (MIM-AF). RNU6-normalized levels of MiR92b-3p were quantified by RT-qPCR at 24 and 48 h after delivery relative to PBS (at 24 h) or to IVF (at 48 h) as control groups. Two individual biological replicates were performed in each variant. Horizontal lines denote means. Please refer to "Fish and experimental design" in the Materials and methods section for more details concerning particular experimental groups of fish and the time-points at which the samples were collected. (A color version of this figure is available in the online journal.)

in the fish treated with MIM-1.0 (Supplementary Figure 3). Likewise, no distinct differences were found in plasma levels of these both miRNAs (MiR92b-3p and MiR122-5p) between the control groups, i.e. PBS-injected fish after 24 h and IVF-injected fish after 48 h of the treatment (Supplementary Figure 3).

Then, we screened the MiR92b-3p levels in several whitefish tissues (Figure 1). At 24 h of treatment, the level of the miRNA in the liver was notably higher in fish that had been injected with the mimic (either MIM-1.0 or MIM-AF) than in those injected with PBS, and the levels of MiR92b-3p remained higher in this organ after 48 h. With the exception of MiR92b-3p in the brain, levels of this miRNA in other tissues were also markedly elevated during 48 h of the treatment, with the highest levels in the spleen (>700-fold). MiR92b-3p level found after 48 h in the examined organs, except the brain of fish exposed for 48 h to the mimic at a dose of 0.3 mg·kg^{-1} (MIM-0.3) was noticeably lower than in these tissues of fish that had been injected with the mimic at the higher dose (i.e. MIM-1.0). Interestingly, the estimated level of MiR92b-3p in the heart was lower in the MIM-0.3 fish than in control fish (IVF), but we cannot rule out the possibility that this difference is due to random variation between fishes. Further studies would help to improve the precision of this estimate.

After detecting differences in the MiR92b-3p levels in tissues after mimic treatment, we looked further at the localization of the miRNA agent in cells by injecting fish with a synthetic 3′-labeled (Alexa Fluor 555) MiR92b-3p mimic. In the liver, 24 h after injection, the orange fluorescence was found around the sinusoids as well as in cytoplasm and nuclei of parenchymal cells (Figure 2(a) to (d)). The fluorescent material formed a continuous layer on the sinusoidal domain of hepatocytes. The thickness of this layer and intensity of its fluorescence differed between sinusoids, and in some sinusoids it was lacking. In the vast majority of hepatocytes, florescence was observed in a form of round, small spots, located mainly in the cytoplasm of the bile domains of hepatocytes. Sporadically, cells with intensively fluorescent, round nuclei were found. They were usually situated between hepatocytes with non-fluorescent nuclei and polygonal or elongated in shape. Their cytoplasm showed variable fluorescence, from the background level

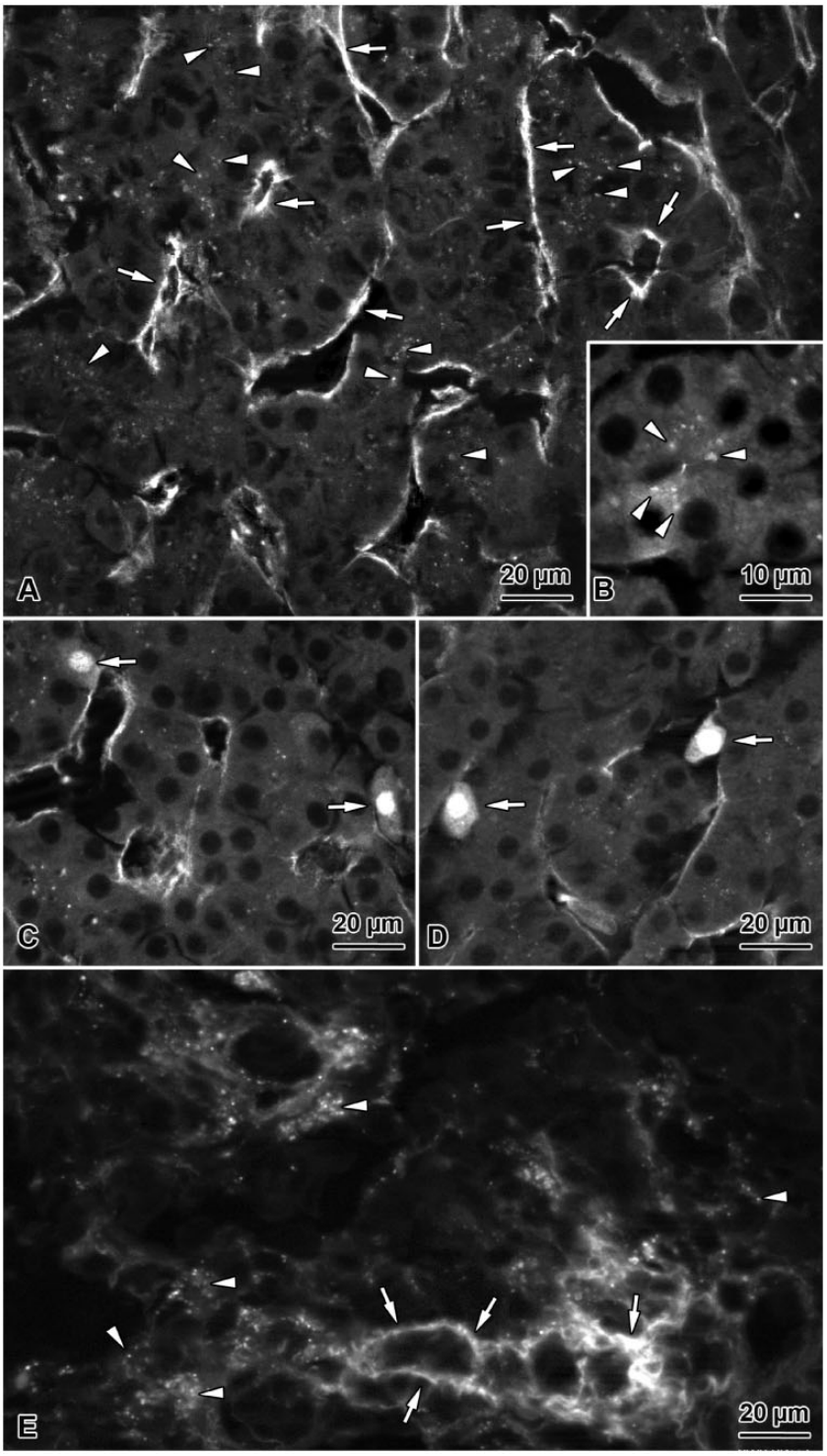

Figure 2. Localization of fluorescent material in the liver (a, b, c, d) and spleen (e) of fish 24 h after peritoneal injection of MiR92b-3p mimic 3′-labeled with Alexa Fluor 555 at a dose of 1 mg·kg^{-1} body weight (MIM-AF). (a) Fluorescence around the liver sinusoids (arrows) and in hepatocyte cytoplasm (arrow heads). (b) Round, fluorescent structures (arrow heads) located in cytoplasm of the bile domains of hepatocytes. (c, d) Cells with intensively fluorescent, round nuclei (arrows) situated between hepatocytes with non-fluorescent nuclei. (e) Fluorescence around the large blood vessels (arrows) and in the processes of intestinal cells in the red pulp (arrow heads).

to moderately intensive. In the spleen, the fluorescence was much more intensive than in the liver. It was observed around the large blood vessels located in the red pulp and in the long, fine cell processes situated in the splenic cords (Figure 2(e)). No fluorescence was observed in the brain, including the cerebrum and cerebellum, neither the fluorescent material was detected in the heart muscle. Together, these results indicate that MiR92b-3p mimic was effectively delivered into the liver and the spleen of the injected fish.

Mimic effects

MiR92b-3p mimic may reduce mRNA expression of its potential target genes. To check if the MiR92b-3p mimic achieved functionality, we measured mRNA expression levels of its putative target genes in whitefish: p53 tumor suppressor, its downstream effector, cdkn1a, and proliferating cell nuclear antigen, pcna (Figure 3). After 24 h of the treatment, no significant differences were found in mRNA expression of the target genes between the control fish (PBS) and those injected with MiR92b-3p mimic (MIM-1.0 and MIM-AF; $P > 0.05$). However, although small number of fish hindered determination of statistically significant differences, the mRNA expression of the target genes was approximately 50% lower 48 h after treatment, which suggests that MiR92b-3p may be involved in negative regulation of their expression.

MiR92b-3p mimic altered mRNA expression profile in the liver. To investigate the possibility that applying a transfection reagent we used to deliver MiR92b-3p mimic into the liver—in addition to the mimic alone—might alter a cell transcriptome of the organ, we performed a transcriptomic study on six liver samples, from the control (PBS), carrier (IVF) and the treated (MIM-1.0) whitefish. Indeed, 48 h after treatment with the mimic, a total of 2637 genes were differentially expressed (DEGs) in the liver ($P < 0.01$; Figure 4). While the three groups examined shared similarities in gene expression, they also differed in the numbers and composition of unique DEGs in pairwise comparisons, at cutoff value of $P < 0.01$. There were 355, 468, and 1046 unique mRNA transcripts in the IVF_MIM-1.0, IVF_PBS, and PBS_MIM-1.0 groups, respectively (Figure 4). In each pairwise comparison, more genes were down-regulated than up-regulated (Figure 4). These results suggested that following administration of the IVF as a carrier, some off-target effects, not related to the mimic activity may have occurred.

Potential role of differentially expressed mRNAs. To better characterize the individual effects of the MiR92b-3p mimic, we further pooled control PBS and IVF samples and re-analyzed against the MIM-1.0 group for DEG discovery. The analysis revealed that of the 772 found differentially expressed between mimic and pooled control samples at a $P < 0.01$, a total of 673 genes belonged to functional panels related to: cellular processes and signaling (312), information storage and processing (143), and metabolism (131), whereas 87 encoded poorly characterized proteins. Unsupervised hierarchical clustering segregated pooled control (PBS+IVF) and mimic samples based on treatment assignment and expression difference at $P < 0.001$ (Supplementary Table 3), suggesting a common transcriptional consequence in response to MiR92b-3p transfection (Figure 5(a)). We found that among aberrantly expressed genes were those involved in, for example, pathways for carbohydrate metabolism (down-regulated phosphoglucomutase 1;

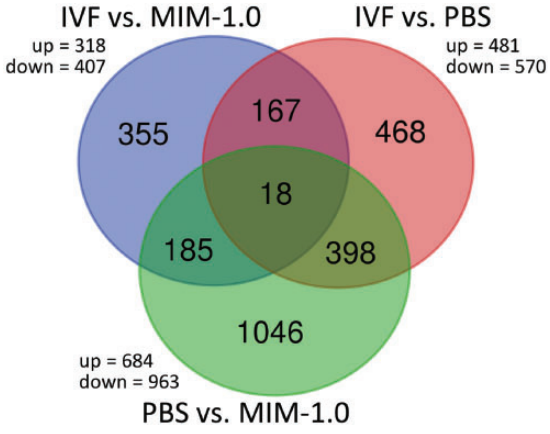

Figure 4. Venn diagram illustrating the relationship between sets of differentially down- or up-regulated genes in the study. There were 355, 468, and 1046 unique mRNA transcripts in the IVF vs. MIM-1.0, IVF vs. PBS, and PBS vs. MIM-1.0 comparisons, respectively. (A color version of this figure is available in the online journal.)

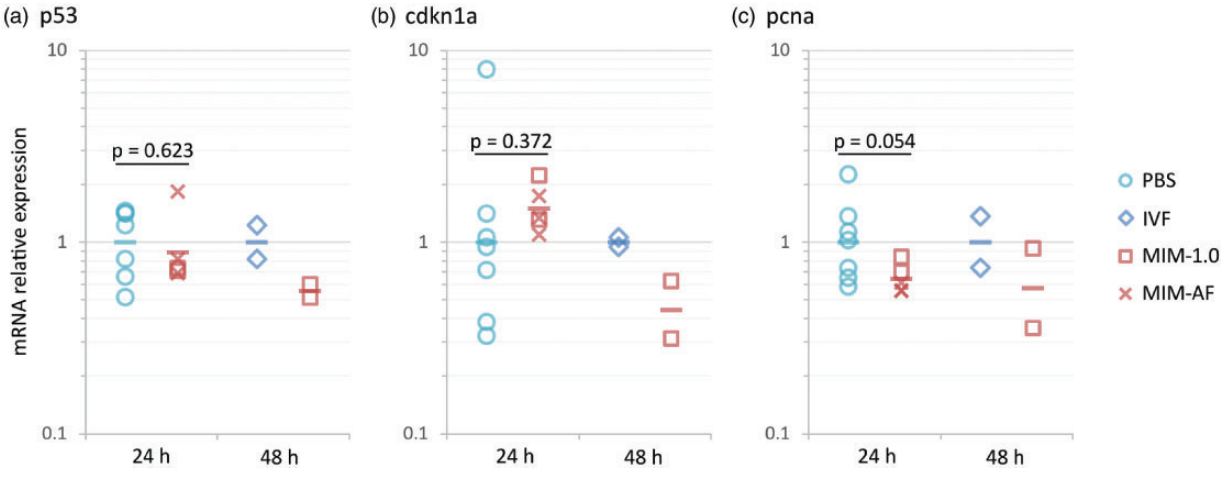

Figure 3. mRNA expression of (a) p53, (b) cdkn1a, and (c) pcna in the liver of whitefish after 24 and 48 h of exposure to the MiR92b-3p mimic at a dose of 1 mg·kg^{-1} body weight (MIM-1.0 and/or MIM-AF). Data were normalized to rpl19 as an endogenous reference, relative to PBS (at 24 h) or to IVF (at 48 h) as control groups. Points indicate individual biological replicates in each variant, whereas horizontal lines denote means. Differences between the two experimental groups (PBS vs. MIM-1.0+MIM-AF) were assessed using a two-tailed Welch's *t*-test. (A color version of this figure is available in the online journal.)

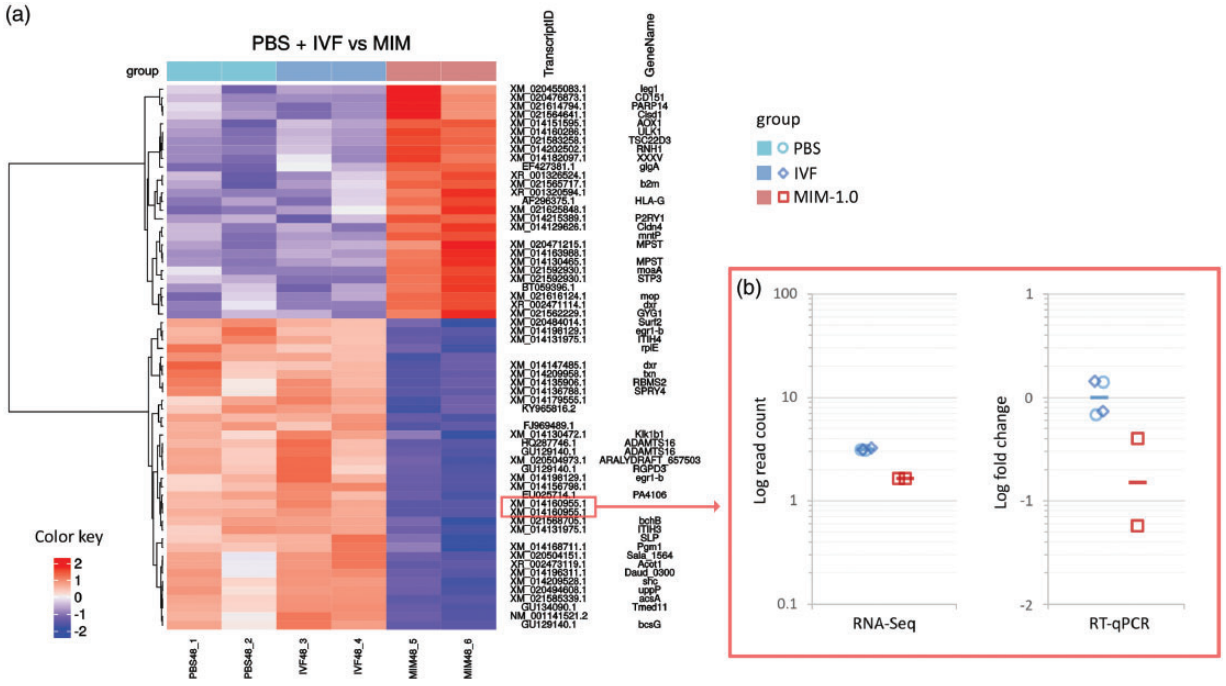

Figure 5. Differentially expressed genes in liver cells transfected with MiR92b-3p mimic at a dose of 1 mg·kg^{-1} body weight (MIM-1.0) and a pooled control of fish injected with phosphate saline (PBS) and fish injected with Invivofectamine vehicle (IVF). (a) Heat map of 63 differentially expressed genes based on unadjusted *t*-test *P*-values ($P < 0.001$), providing an overall picture of the impact of MiR92b-3p mimic injection on the liver cell transcriptome. (b) Changes in the *cdo1* gene expression (Log fold change) assessed in liver using an RNA-Seq method (left panel) and qPCR (right panel) in pooled control (blue circles and diamonds) and mimic treated whitefish (red squares). Horizontal lines in the panels indicate mean values of expression ($n = 4, 2$) in control and mimic-treated groups, respectively, and normalized by rpl19. (A color version of this figure is available in the online journal.)

pgm1), glycogenesis (up-regulated glycogen synthase; *glga*), pentose phosphate (up-regulated aldehyde oxidoreductase; *mop*), or transmembrane sugar transport (elevated sugar transport protein; *stp3*, Figure 5(a)). These perturbations did not prompt global, specific silencing but instead produced significant changes in a finite number of genes that occurred 48 h after transfection of the mimic.

To further confirm the RNA-Seq data, we selected one gene and designed a qPCR study that re-analyzed the level of whitefish cysteine dioxygenase 1 mRNA, cdo1 (the mRNA sequence has been annotated in GenBank under the No. MH818218), the expression of which was the most significantly reduced after transfection with the MiR92b-3p agent ($P = 7.11 \times 10^{-7}$; Supplementary Table 3). The *CDO1* gene has been previously linked with the production of sulfate and taurine and intracellular redox regulation in mammals[22] and our data, both RNA-Seq and qPCR, confirmed significant reduction of its expression 48 h after treatment with the miRNA agent (Figure 5(b)).

To globally analyze the biological significance of the differentially abundant mRNAs potentially involved in regulatory pathways, we performed an enrichment analysis. As shown in Figure 6, after 48 h of the MiR92b-3p transfection, the most frequent terms were "DNA-templated," "transcription," "regulation" suggesting perturbations in biological processes of transcription regulation, and "membrane," "cytoplasm" which may indicate main cellular components involved. The Gene Ontology analysis revealed also that aberrant molecular functions inferred from transcript levels in control and treated samples

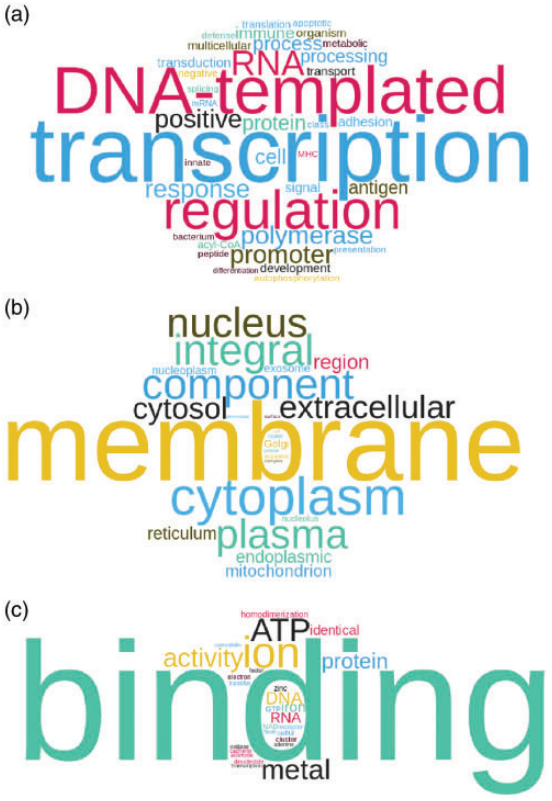

Figure 6. Graphical representation of the 20 most frequent Gene Ontology terms in each of three categories: (a) biological process, (b) cellular component, and (c) molecular function. This graph was generated using TagCloud software (https://www.wordclouds.com). (A color version of this figure is available in the online journal.)

primarily enriched terms "binding", " ion," and "metal" (Figure 6).

The treatment did not cause any distinct toxic effects in short-term. *In vivo* transfection with synthetic oligonucleotides may result in non-specific or even toxic effects in the challenged animals (e.g. Straarup *et al.*[23]). In order to monitor for these potential effects of the treatment with MiR92b-3p mimic, we first performed histological and ultrastructural analysis of the liver. The liver parenchyma in control fish (PBS) was formed by anastomosing tubules of hepatocytes, separated from each other by sinusoids. Hepatocytes were cubic or polygonal in shape and contained usually single, euchromatin-rich nucleus with prominent nucleolus and irregularly distributed spots of heterochromatin. The cytoplasm was unevenly stained with H&E method and comprised both acidophilic and basophilic areas. Vacuoles or lipid droplets were sparse. No differences were observed in histological structure of the liver between this control group and other groups of fish (Supplementary Figure 4).

No distinct differences were also found in the hepatocytes' ultrastructure between the control groups and the treatment groups (Supplementary Figures 5 and 6). In all studied fish, hepatocyte nuclei were round or oval in shape and did not form deep invaginations of the nuclear envelope. The plasma membrane covering the sinusoidal domain formed very long microvilli, filling the perivascular space. The cytoplasm of the sinusoidal domain contained long, parallel oriented cisterns of granular endoplasmic reticulum and numerous glycogen particles forming accumulations of variable size. Dense or myeloid bodies were observed close to or inside the glycogen accumulations. The smooth endoplasmic reticulum, dictyosomes of the Golgi apparatus, lysosomes and small accumulations of glycogen particles were located on the bile domain. The cytoplasm around the bile canaliculi contained many vesicles with variable size and content. Mitochondria with electron dense matrix and prominent cristae, frequently elongated were randomly dispersed in hepatocyte cytoplasm. The lipid droplets were usually sparse.

Finally, to support the histological and ultrastructural analyses, the fishes' blood collected after 48 h of the treatment was examined for selected hematological and biochemical markers (Supplementary Table 4). Except of the glucose (GLU) level, which was decreased in the IVF, MIM-0.3 and MIM-1.0 groups in comparison to fish injected PBS, there were no apparent differences in the examined hematological and biochemical indices.

To summarize the above results, histopathological and ultrastructural analyses did not show any major changes in the livers of the exposed fish, and the experimental groups did not differ in terms of hematological and biochemical measurements of the fishes' blood, confirming that the fishes did not exhibit any discernible toxic effects of the treatment.

Discussion

An essential step in miRNA-mediated therapeutics is the delivery of synthetic snippets of RNA to the right cells, to silence or replace miRNAs. In order to reach their site of action, the cytosol, synthetic miRNA need to overcome a number of barriers that stand in their way.[24,25] Here, we confirmed that after intraperitoneal injection, miRNA mimic entered the blood circulation of the fish and was distributed to the organs. In the organs, the traveling synthetic miRNA extravasated from the blood vessels and was associated with target cells, most likely through the process involving the passage of the miRNA agent to the intersticium, overcoming the endothelial barrier, followed by uptake by endocytotic mechanisms.[26] It is known that the endothelial barrier determines distribution into organs,[27] and our results are consistent with this finding. The liver, as well as the lymphoid tissue and hematopoietic organs, contain sinusoidal, discontinuous capillaries. These capillaries lack a diaphragm over the pore, and are therefore more permeable, allowing the exchange of macromolecules.[25] Thus, miRNA delivery systems may work better with the liver and the spleen than with the brain and heart. Our findings support the view that in addition to intravenous injections commonly used in studies on mammals, the injection of a synthetic mimic into the peritoneal cavity of fish is a good alternative method for introducing these substances to the blood stream in these animals.

The development of miRNA replacement strategies for achieving knockdown is based upon the disease suppressive activity of some of the known miRNAs. Some of miRNA replacement for achieving knockdown in fish conducted so far, have shown that delivering synthetic miRNAs is also an attractive tool for exploring gene functions in various biological and immunological processes by elucidating the roles of particular miRNAs in the regulation of cellular pathways.[6,7] MIR92b-3p, which confers pro-proliferative and anti-apoptotic phenotypes, by interfering with various tumor suppressor genes in mammals,[28] has become an interesting object of study in fish. We recently reported expression of MIR92b-3p to be substantially reduced in the liver of a MC-LR challenged group of whitefish,[11] and we suggested that this miRNA reduction is linked to a yet unknown molecular pathway leading to regeneration of the damaged liver structure.[10] If MiR92b-3p contributed to this process, it is possible that MiR92b-3p synthetic agent, delivered to liver cells, could potentially result in down-regulation of genes that control cell proliferation during regeneration of the MC-LR-damaged liver. Here, we explored this possibility by studying the molecular effects induced by MiR92b-3p mimics on both individual genes and global transcriptional pathways in the liver of healthy fish. We predicted that p53, cdkn1a, and pcna expression would be reduced after the MiR92b-3p mimic transfection, because in previous works, transcript levels of the three genes were found up-regulated in whitefish liver after MC-LR exposure.[10,11,29,30] What is more, the preliminary screening of their 3′UTRs confirmed the presence of MiR92b-3p response elements, suggesting their functional relationships. Indeed, reduction of gene expression, as shown in Figure 3, may further support the idea that they constitute miRNA/mRNA regulatory pairs.

The role of p53 and its downstream effector cdkn1a in triggering responses in cells and organs challenged by various stress stimuli (e.g. chemotherapeutics, ultraviolet or γ-irradiation, hepatectomy) has been supported by data obtained from several *in vitro* and *in vivo* models.[31–33] Our results add to these previous studies by suggesting that MiR92b-3p may be involved in the regulation of the cell signaling processes. In mammals and birds, the transcriptional activation and protein stability of cdkn1a are tightly controlled by several distinct mechanisms,[34] and microRNAs play a role in these processes.[35] CDKN1A/P21Cip1 is an important effector that acts by inhibiting CDK activity in p53-mediated cell cycle arrest in response to various agents.[36] For example, when genotoxic events, such as X-rays, evoke an increase in cellular p53 levels in mammals, the levels of P21Cip1 protein subsequently increase.[37] What is more, CDKN1A protein is able to interact with proliferating cell nuclear antigen (PCNA),[38] a processivity factor of DNA polymerase, and thus it plays a role in the control the G1 to S phase transition. Thus, the potential ability of MiR92b-3p mimic to reduce expression *in vivo* of either p53, cdkn1a, and/ or pcna may have important applications in fish functional genomics experiments. The MiR92b-3p mimic transfection may be, for instance, a useful tool in studies attempting to analyze signal transduction pathways after treatment with genotoxic compounds, such as MC-LR, or in assessing the genotoxicity of drug candidates.

After finding reduced expression of the putative target genes, we were curious about whether *in vivo* transfection of liver cells with MiR92b-3p mimic modulates expression of other genes, and which molecular processes and cellular components are engaged. KOG and GO analyses revealed modulation of several pathways involved in the control of cellular processes and signaling, information storage and processing and metabolism. One of the most affected biological processes was transcription regulation, which is consistent with previous reports demonstrating that transfection of small RNAs globally perturbs gene regulation.[39] Similarly, indication of involvement of pathways related to membranes after mimic transfection is not surprising since it was demonstrated that, to be active, the synthetic RNAi agent needs to overcome the cell membrane barrier, then localize into an endosomal vesicle and finally, escape from it to achieve functionality.[40] What is more, these dynamic processes of cellular uptake and intracellular trafficking of miRNA agents are strongly influenced by delivery vehicle.[25]

The mimic injection into peritoneal cavity of fish could have had effects on metabolic processes in liver cells, as seen in aberrant molecular functions revealed by transcription and gene ontology enrichment analysis. Notably, the (metal, ion) binding activity was perturbed in MiR92b-3p treated fish, as some of their important metabolic genes were aberrantly modulated. Cysteine dioxygenase (CDO) in mammals is expressed in liver, pancreas, kidney, lung, and white and brown adipose tissues, allowing these tissues to metabolize excess cysteine to sulfate and taurine. Because elevated levels of cysteine have been shown to be both cytotoxic and neurotoxic, being reported in human individuals with a variety of autoimmune and neurodegenerative diseases,[41] the reduced levels of cdo1 mRNA reported here may indicate temporal perturbation of the cysteine homeostasis in the liver of fish injected with miRNA agent. At the moment it is unclear, whether the cdo 3′UTR is a functional target for MiR92b-3p, or the treatment with the mimic produced unwanted off-target effect, i.e. unintended down-regulation of cdo1 mRNAs through a partial sequence seed match between the miRNA and target, or the effects observed here are distinct and involve other regulatory circuits. Further studies, both reporter and functional ones, will be required to confirm functionality of this putative regulatory miRNA/mRNA pair. By proving this, the role of MIR92b-3p would be expanded beyond conferring pro-proliferative and anti-apoptotic phenotypes,[28] to include one of intracellular metabolism regulation.

In conclusion, in this report we provide the first data on synthetic miRNA delivery, cellular uptake, and gene knockdown efficiency for MiR92b-3p, a microRNA potentially involved in microcystin-LR-induced liver injury in fish. Our results indicate that the MiR92b-3p mimic was effectively delivered to the spleen and the liver of the injected fish (it was localized in the cells as small vesicles) and likely achieved functionality. Furthermore, we showed that the short-term treatment with the synthetic mimic did not cause any distinct toxic effects in the challenged fish. Thus, the described methodology of miRNA mimic delivery has utility for the study of miRNA-dependent silencing mechanisms during MILI and for the development of both miRNA diagnostic markers and therapeutic targets in fish liver injury.

Authors' contributions: PB and MW prepared the concept of this project; MW, SD, and MF supervised the hatchery operations and collected the samples; PG performed the biochemical measurements; BL performed the histological and ultrastructural analyses; MF, PB, MW performed the gene expression analysis; PB, MW and PG performed the statistical analyses; PB and MF examined the RNA-Seq data; PB, MW and BL worked on the results interpretation and wrote the manuscript; MW and BL prepared the graphical design. All authors had approved the final version of manuscript before its submission.

DECLARATION OF CONFLICTING INTERESTS

The author(s) declared no potential conflicts of interest with respect to the research, authorship, and/or publication of this article.

FUNDING

The project was funded by the National Science Centre of Poland (decision number: 2016/21/B/NZ9/03566).

ORCID iD

Maciej Woźny http://orcid.org/0000-0001-5201-2925
Maciej Florczyk http://orcid.org/0000-0003-2277-312X

REFERENCES

1. Ha M, Kim VN. Regulation of microRNA biogenesis. *Nat Rev Mol Cell Biol* 2014;**15**:509–24

2. Lam JKW, Chow MYT, Zhang Y, Leung SWS. siRNA versus miRNA as therapeutics for gene silencing. *Mol Ther* 2015;**4**:e252
3. Krützfeldt J, Rajewsky N, Braich R, Rajeev KG, Tuschl T, Manoharan M, Stoffel M. Silencing of microRNAs in vivo with antagomirs. *Nature* 2005;**438**:685–9
4. Lanford RE, Hildebrandt-Eriksen ES, Petri A, Persson R, Lindow M, Munk ME, Kauppinen S, Orum H. Therapeutic silencing of microRNA-122 in primates with chronic hepatitis C virus infection. *Science* 2010;**327**:198–201
5. Jiangpan P, Qingsheng M, Zhiwen Y, Tao Z. Emerging role of microRNA in neuropathic pain. *Curr Drug Metab* 2016;**17**:336–44
6. Cui J, Gao Y, Chu Q, Bi D, Xu T. miRNA-8159 is involved in TLR signaling pathway regulation after pathogen infection by direct targeting TLR13 in miiuy croaker. *Fish Shellsh Immunol* 2017;**66**:531–9
7. Huang H, Zhang K, Zhou Y, Ding X, Yu L, Zhu G, Guo J. MicroRNA-155 targets cyb561d2 in zebrafish in response to fipronil exposure. *Environ Toxicol* 2016;**31**:877–86
8. Mennigen JA, Martyniuk CJ, Seiliez I, Panserat S, Skiba-Cassy S. Metabolic consequences of microRNA-122 inhibition in rainbow trout, *Oncorhynchus mykiss*. *BMC Genom* 2014;**15**:70
9. Hoppe B, Pietsch S, Franke M, Engel S, Groth M, Platzer M, Englert C. MiR-21 is required for efficient kidney regeneration in fish. *BMC Dev Biol* 2015;**15**:43
10. Woźny M, Lewczuk B, Ziókowska N, Gomuka P, Dobosz S, Łakomiak A, Florczyk M, Brzuzan P. Intraperitoneal exposure of whitefish to microcystin-LR induces rapid liver injury followed by regeneration and resilience to subsequent exposures. *Toxicol Appl Pharmacol* 2016;**313**:68–87
11. Brzuzan P, Florczyk M, Łakomiak A, Woźny M. Illumina sequencing reveals aberrant expression of microRNAs and their variants in whitefish (*Coregonus lavaretus*) liver after exposure to microcystin-LR. *PLoS One* 2016;**11**:e0158899
12. Biggar KK, Wu C-W, Storey KB. High-throughput amplification of mature microRNAs in uncharacterized animal models using polyadenylated RNA and stem-loop reverse transcription polymerase chain reaction. *Anal Biochem* 2014;**462**:32–4
13. Florczyk M, Brzuzan P, Łakomiak A, Jakimiuk E, Woźny M. Microcystin-LR-triggered neuronal toxicity in whitefish does not involve MiR124-3p. *Neurotox Res* 2019;**35**:29–40
14. Florczyk M, Brzuzan P, Krom J, Woźny M, Łakomiak A. miR-122-5p as a plasma biomarker of liver injury in fish exposed to microcystin-LR. *J Fish Dis* 2016;**39**:741–51
15. Pasquier J, Cabau C, Nguyen T, Jouanno E, Severac D, Braasch I, Journot L, Pontarotti P, Klopp C, Postlethwait JH, Guiguen Y, Bobe J. Gene evolution and gene expression after whole genome duplication in fish: the PhyloFish database. *BMC Genom* 2016;**17**:368
16. Rehmsmeier M. Fast and effective prediction of microRNA/target duplexes. *RNA* 2004;**10**:1507–17
17. Bolger AM, Lohse M, Usadel B. Trimmomatic: a flexible trimmer for illumina sequence data. *Bioinformatics* 2014;**30**:2114–20
18. Haas BJ, Papanicolaou A, Yassour M, Grabherr M, Blood PD, Bowden J, Couger MB, Eccles D, Li B, Lieber M, MacManes MD, Ott M, Orvis J, Pochet N, Strozzi F, Weeks N, Westerman R, William T, Dewey CN, Henschel R, LeDuc RD, Friedman N, Regev A. De novo transcript sequence reconstruction from RNA-seq using the trinity platform for reference generation and analysis. *Nat Protoc* 2013;**8**:1494–512
19. Robinson MD, McCarthy DJ, Smyth GK. edgeR: a bioconductor package for differential expression analysis of digital gene expression data. *Bioinformatics* 2010;**26**:139–40
20. Koonin EV, Fedorova ND, Jackson JD, Jacobs AR, Krylov DM, Makarova KS, Mazumder R, Mekhedov SL, Nikolskaya AN, Rao BS, Rogozin IB, Smirnov S, Sorokin AV, Sverdlov AV, Vasudevan S, Wolf YI, Yin JJ, Natale DA. A comprehensive evolutionary classification of proteins encoded in complete eukaryotic genomes. *Genome Biol* 2004;**5**:R7
21. Svobodova Z, Pravda D, Palackova J, Svobodová Z, Paláčková J. *Unied methods of haematological examination of sh*. Vodnany, Czech Republic: Research Institute of Fish Culture and Hydrobiology, 1991, p.31
22. Dominy JE, Hwang J, Stipanuk MH. Overexpression of cysteine dioxygenase reduces intracellular cysteine and glutathione pools in HepG2/C3A cells. *Am J Physiol Endocrinol Metab* 2007;**293**:E62–9
23. Straarup EM, Fisker N, Hedtjärn M, Lindholm MW, Rosenbohm C, Aarup V, Hansen HF, Ørum H, Hansen JBR, Koch T. Short locked nucleic acid antisense oligonucleotides potently reduce apolipoprotein B mRNA and serum cholesterol in mice and non-human primates. *Nucleic Acids Res* 2010;**38**:7100–11
24. Wang J, Lu Z, Wientjes MG, Au JL-S. Delivery of siRNA therapeutics: barriers and carriers. *AAPS J* 2010;**12**:492–503
25. Lorenzer C, Dirin M, Winkler A-M, Baumann V, Winkler J. Going beyond the liver: progress and challenges of targeted delivery of siRNA therapeutics. *J Controll Rel* 2015;**203**:1–15
26. Dominska M, Dykxhoorn DM. Breaking down the barriers: siRNA delivery and endosome escape. *J Cell Sci* 2010;**123**:1183–9
27. Takakura N, Mahato N, Hashida N. Extravasation of macromolecules. *Adv Drug Deliv Rev* 1998;**34**:93–108
28. Zhuang LK, Yang YT, Ma X, Han B, Wang ZS, Zhao QY, Wu LQ, Qu ZQ. MicroRNA-92b promotes hepatocellular carcinoma progression by targeting Smad7 and is mediated by long non-coding RNA XIST. *Cell Death Dis* 2016;**7**:e2203
29. Brzuzan P, Woźny M, Ciesielski S, Łuczyński MK, Góra M, Kuźmiński H, Dobosz S. Microcystin-LR induced apoptosis and mRNA expression of p53 and cdkn1a in liver of whitefish (*Coregonus lavaretus L.*). *Toxicon* 2009;**54**:170–83
30. Brzuzan P, Woźny M, Wolińska L, Piasecka A. Expression profiling in vivo demonstrates rapid changes in liver microRNA levels of whitefish (Coregonus lavaretus) following microcystin-LR exposure. *Aquat Toxicol* 2012;**122–123**:188–96
31. Rodriguez R, Meuth M. Chk1 and p21 cooperate to prevent apoptosis during DNA replication fork stress. *Mol Biol Cell* 2006;**17**:402–12
32. Liu W-H, Zhao Y-S, Gao S-Y, Li S-D, Cao J, Zhang K-Q, Zou C-G. Hepatocyte proliferation during liver regeneration is impaired in mice with methionine diet-induced hyperhomocysteinemia. *Am J Pathol* 2010;**177**:2357–65
33. Ouhtit A, Ismail MF, Othman A, Fernando A, Abdraboh ME, El-Kott AF, Azab YA, Abdeen SH, Gaur RL, Gupta I, Shanmuganathan S, Al-Farsi YM, Al-Riyami H, Raj MHG. Chemoprevention of rat mammary carcinogenesis by spirulina. *Am J Pathol* 2014;**184**:296–303
34. Foertsch F, Teichmann N, Kob R, Hentschel J, Laubscher U, Melle C. S100A11 is involved in the regulation of the stability of cell cycle regulator p21 $^{CIP\ 1/WAF\ 1}$ in human keratinocyte HaCaT cells. *FEBS J* 2013;**280**:3840–53
35. Ivanovska I, Ball AS, Diaz RL, Magnus JF, Kibukawa M, Schelter JM, Kobayashi SV, Lim L, Burchard J, Jackson AL, Linsley PS, Cleary MA. MicroRNAs in the miR-106b family regulate p21/CDKN1A and promote cell cycle progression. *Mol Cell Biol* 2008;**28**:2167–74
36. Dulić V, Kaufmann WK, Wilson SJ, Tlsty TD, Lees E, Harper JW, Elledge SJ, Reed SI. p53-dependent inhibition of cyclin-dependent kinase activities in human fibroblasts during radiation-induced G1 arrest. *Cell* 1994;**76**:1013–23
37. Vousden KH, Lu X. Live or let die: the cell's response to p53. *Nat Rev Cancer* 2002;**2**:594–604
38. Gulbis JM, Kelman Z, Hurwitz J, O'Donnell M, Kuriyan J. Structure of the C-terminal region of p21(WAF1/CIP1) complexed with human PCNA. *Cell* 1996;**87**:297–306
39. Khan AA, Betel D, Miller ML, Sander C, Leslie CS, Marks DS. Transfection of small RNAs globally perturbs gene regulation by endogenous microRNAs. *Nat Biotechnol* 2009;**27**:549–55
40. Juliano RL, Carver K, Cao C, Ming X. Receptors, endocytosis, and trafficking: the biological basis of targeted delivery of antisense and siRNA oligonucleotides. *J Drug Target* 2013;**21**:27–43
41. Stipanuk MH, Ueki I, Dominy JE, Simmons CR, Hirschberger LL. Cysteine dioxygenase: a robust system for regulation of cellular cysteine levels. *Amino Acids* 2009;**37**:55–63

(Received September 17, 2018, Accepted December 21, 2018)